Determination of QCD phase diagram from the imaginary chemical potential

Yuji Sakai[†], Kouji Kashiwa[†], Hiroaki Kouno[‡], Masanobu Yahiro[†]
Department of Physics, Kyushu University[†],
Department of Physics, Saga University[‡],

1 Introduction

The QCD phase diagram is essential for understanding not only natural phenomena such as compact stars and the early universe but also laboratory experiments such as relativistic heavy-ion collisions. Unfortunately, quantitative calculations of lattice QCD (LQCD) have the well-known sign problem when the chemical potential (μ) is real. So far, several approaches have been proposed to circumvent the difficulty; one is the analytic continuation to real chemical potential ($\mu_{\rm R}$) from imaginary chemical potential ($\mu_{\rm I}$) [1].

As an approach complementary to LQCD, we can consider effective models such as the Nambu–Jona-Lasinio (NJL) model and the Polyakov-loop NJL (PNJL) model [2,3]. In the NJL-type models, the input parameters are determined at $\mu = 0$. It is then highly nontrivial whether the models predict properly dynamics of QCD at finite $\mu_{\rm R}$. This should be tested from QCD. Fortunately, this is possible at $\mu_{\rm I}$, since LQCD has no sign problem there.

The QCD partition function $Z(\theta)$ at $\mu_{\rm I} = i\theta T$ has a periodicity $Z(\theta) = Z(\theta + 2\pi/3)$, showing that $Z(\theta + 2\pi/3)$ is transformed into $Z(\theta)$ by the $\mathbb{Z}_3$ transformation with integer k [4]. This means that QCD is invariant under a combination of the $\mathbb{Z}_3$ transformation and a parameter transformation $\theta \to \theta + 2\pi/3$,

$$q \to Uq, \quad A_\nu \to UA_\nu U^{-1} - \frac{i}{g}(\partial_\nu U)U^{-1}, \quad \theta \to \theta + 2\pi/3, \tag{1}$$

where $U(x,\tau)$ are elements of $SU(3)$ with $U(x,1/T) = \exp(-2i\pi k)U(x,0)$ and q is the quark field. We call this combination the extended $\mathbb{Z}_3$ transformation. Thus, $Z(\theta)$ has the extended $\mathbb{Z}_3$ symmetry, and hence quantities invariant under this transformation have the Roberge-Weiss (RW) periodicity.

At the present stage, the PNJL model is only a realistic effective model that possesses both the extended $\mathbb{Z}_3$ symmetry and chiral symmetry. This property guarantees that the phase diagram evaluated by the PNJL model has the RW periodicity at $\mu_{\rm I}$, and therefore makes it possible to compare the PNJL model with LQCD quantitatively at $\mu_{\rm I}$. If the PNJL model succeeds in reproducing the lattice data, we may think that the PNJL model will predict, with high reliability, the QCD phase structure at $\mu_{\rm R}$ [5].

2 Comparision between PNJL and LQCD

The two-flavor PNJL Lagrangian in Euclidean spacetime is

$$\mathcal{L} = \bar{q}(i\gamma_\nu D_\nu - \gamma_4\mu + m_0)q - G_s[(\bar{q}q)^2 + (\bar{q}i\gamma_5\vec{\tau}q)^2] + U_p(\Phi[A], \Phi^*[A], T), \qquad (2)$$

where q denotes the two-flavor quark field, m_0 does the current quark mass, and $D_\nu = \partial_\nu - iA_\nu\delta_{\nu 4}$. In the NJL sector, G_s denotes the coupling constant of the scalar-type four-quark interaction. The Polyakov potential U_p is a function of the Polyakov loop $\Phi = \frac{1}{N_c}\mathrm{tr}_c e^{-iA_4/T}$ and we use the same of Ref. [3], which is fitted to a LQCD simulation in the pure gauge theory at finite T. We use Φ to define the deconfinement phase transition.

The left panel of Fig. 1 shows the phase diagram of the chiral and deconfinement phase transitions in the $\theta - T$ plane, where $T_c = 173$ MeV is the deconfinement temperature at $\theta = 0$. The lattice data are shown with 10% error. The lattice simulations point out that the chiral and the deconfinement phase transition give the same transition temperature within numerical errors in the entire region $0 \leq \theta \leq 2\pi/3$.

The phase diagram has a periodicity of $2\pi/3$ in θ. This is called the RW periodicity [4,5]. The phase diagram is also θ even, because so is Ω. On the dotdashed line going up from an endpoint $(\theta_{RW}, T_{RW}) = (\pi/3, 1.09T_c)$, the quark-number density and the phase of the Polyakov loop are discontinuous [5]. This is called the RW phase transition line.

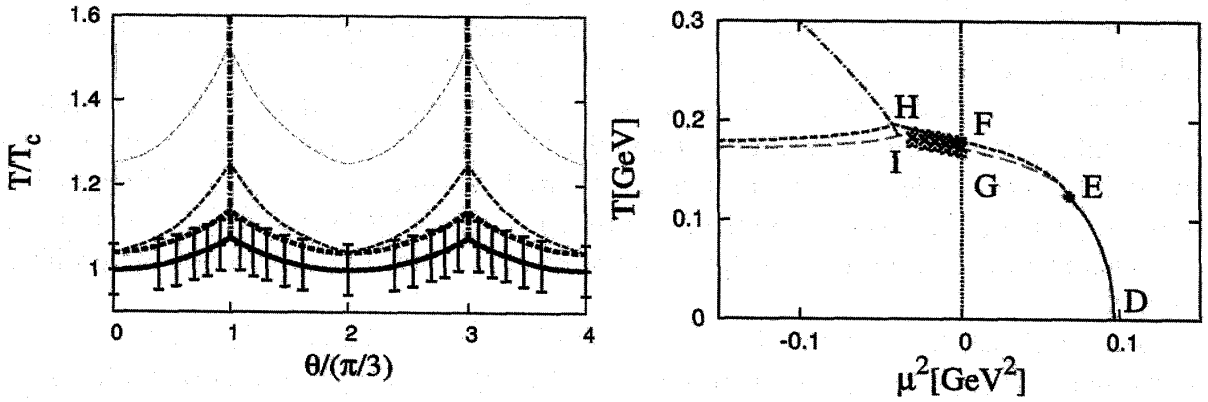

Figure 1: **Left panel;** Phase diagrams of the chiral phase transition at μ_I, calculated with three parameter sets are presented by dashed curves; thin, thick, and bold ones are results of the PNJL calculations with set A, B, and C, respectively. Lattice data [1] are shown with 10% error. The deconfinement phase transition curve (bold solid curve) and the RW phase transition lines (bold dot-dashed lines) calculated with set C are also shown for comparison. **Right panel;** Phase diagram in the real and imaginary chemical potential region. Panels (c) are calculated with the parameter set C. Cross symbols with error bars indicate the lattice data taken from Ref. [1]. Points D-I are explained in the text.

In the left panel of Fig. 1, thin, thick, and bold curves are results of the PNJL calculations with sets A, B, and C, respectively, where set A is the original PNJL, set B is the PNJL with the scalar-type eight-quark interaction, $G_{s8}[(\bar{q}q)^2 + (\bar{q}i\gamma_5\vec{\tau}q)^2]^2$, and set C is futhermore with the vector-type four-quark interaction, $G_v(\bar{q}\gamma_\nu q)^2$. These concrete values are mentioned in third of the reference [5].

Only the PNJL calculations with set C can reproduce the lattice result [1] for both the chiral and deconfinement phase transition temperatures within numerical errors in the entire region $0 \leq \theta \leq 2\pi/3$.

3 Prediction of the phase diagram at real μ

Finally, we predict the phase diagram at real μ by using the PNJL model. The left panel of Fig. 1 represents the phase diagrams in the $\mu^2 - T$ plane predicted by the PNJL calculations with parameter set C. On the solid curve between points E and D, both the first-order chiral and deconfinement phase transitions take place simultaneously, and hence point E is the critical endpoint of these phase transitions. The dotdashed curve moving up from point I represents the RW phase transition of first order, and then point I is the critical endpoint of the RW phase transition. The dashed curve between points H and E means the crossover chiral phase transition, while the long-dashed curve between points I and E does the crossover deconfinement phase transition. Point F (G) is a crossing point between the dashed (longdashed) curve and the $\mu = 0$ line. Cross symbols with error bars indicate LQCD data [1].

The right panel of Fig. 1 is most reliable, since the PNJL result with parameter sets C is consistent with the LQCD one [1] in the $\mu^2 < 0$ region. The critical endpoint does not disappear in virtue of the eight-quark interaction, even if the vector-type interaction is taken into account.

References

[1] P. de Forcrand and O. Philipsen, Nucl. Phys. **B642**, 290 (2002). L. K. Wu, X. Q. Luo, and H. S. Chen, Phys. Rev. **D76**, 034505 (2007).

[2] K. Fukushima, Phys. Lett. B **591**, 277 (2004); Phys. Rev. D **77**, 114028 (2008).

[3] S. Rößner, C. Ratti, and W. Weise, Phys. Rev. D **75**, 034007 (2007).

[4] A. Roberge and N. Weiss, Nucl. Phys. **B275**, 734 (1986).

[5] Y. Sakai, K. Kashiwa, H. Kouno, and M. Yahiro, Phys. Rev. D **77**, 051901(R) (2008); Phys. Rev. D **78**, 036001 (2008); Phys. Rev. D **79**, 096001 (2009); Y. Sakai, K. Kashiwa, H. Kouno, M. Matsuzaki, and M. Yahiro, Phys. Rev. D **78**, 076007 (2008).

[6] F. Karsch, Lect. notes Phys. **583**, 209 (2002); F. Karsch, E. Laermann, and A. Peikert, Nucl. Phys. B **605**, 579 (2002); M. Kaczmarek and F. Zantow, Phys. Rev. D **71**, 114510 (2005).